Do Fukui Function Maxima Relate to Sites of Metabolism? A Critical Case Study

Michael E. Beck*

Bayer CropScience, Research/Scientific Computing, Agricultural Centre Monheim, D-40789 Monheim, Germany

Received October 15, 2004

The usefulness of local reactivity descriptors for understanding drug metabolism is investigated. Electrophilic Fukui functions are calculated for 18 drugs and 11 agrochemicals and their relation to experimentally observed metabolites is discussed. Maxima of the Fukui functions correspond to major sites of metabolic attack in many examples, facilitating a posteriori understanding of experimental findings. In the second part of the paper, the nature of the electrophilic oxidant species in cytochromes, called "Compound I" (Cpd I), is investigated within the Fukui framework. Nucleophilic Fukui functions are calculated involving the relevant spin states of Cpd I, allowing a more qualitative, intuitive understanding of its reactivity.

INTRODUCTION

Understanding the metabolic fate and behavior of a drug or agrochemical is of crucial importance for the development of such chemicals, as metabolism in conjuction with absorption, distribution, and excretion determines bioavailability, effect, and adverse reactions as well as toxicology of a drug or agrochemical.

Many computational approaches exist for understanding metabolism and/or toxicology a posteriori as well as prospectively. These typically use statistical modeling based on (often topological) molecular descriptors.[1−3]

Cytochromes play an important role in metabolism, as most oxidative metabolic reactions are mediated by these enzymes (see ref 4 and 5 for reviews on experimental and theoretical work). With the availability of X-ray structures of cytochromes, 3D-QSAR models have been developed (for example, see refs 6−9). Another approach is ligand based, predicting the preferred sites of hydrogen abstraction by quantum chemistry (for example, see refs 10 and 11).

The most straightforward, but also most demanding, approach certainly is to model the entire process of cytochrome-mediated hydroxylation quantum chemically.[5,12,13] In the most recent such calculation,[13] which serves as a reference throughout this text, the hydroxylation process has been modeled by coupled quantum/molecular mechanics (QM/MM). These calculations strongly support the "two-state reactivity" model (TSR), in which the putative oxidizing species in the active site of cytochromes,[14] called "Compound I" (Cpd I), is viewed as a radical species of either doublet or quartet spin coupling. The reaction takes place in a two-step so-called rebound mechanism. In the first step, hydrogen is abstracted from the substrate. The activation barrier for this step is slightly lower in the doublet state than in the quartet. In a second step, a hydroxy group is added to the substrate. This step is essentially without a barrier in the doublet but requires some activation in the quartet.

The first and only application of DFT-derived reactivity descriptors to a biological system the author is aware of is[15] where the hard and soft acids and bases (HSAB) principle[16] was applied to inorganic model systems for arsenate reductase and low molecular weight phosphatase.

In this study, Fukui functions[17] are calculated for a number of drugs and agrochemicals for which metabolites are known. It is investigated in how far maxima of these functions can be related to observed metabolites, aiming at establishing rather qualitative rather than quantitative relationships.

In the second part of the paper, Fukui functions are calculated for a model system of Cpd I. The idea behind this is to gain some qualitative, chemically intuitive insight into the nature of this elusive species.

THEORY

Some Results from Conceptional DFT.[17−21] A number of concepts for general chemical reactivity exist, such as the principle of hard and soft acids and bases,[16,22] electronegativity,[23−25] and frontier orbital theory.[26−28] These concepts gained a solid theoretical foundation in density functional theory, namely, through the work of Yang and Parr.[18,17]

Besides its formal beauty, this theory exhibits another nice property: The necessary calculations are rather easy to perform.

Within density functional theory, the chemical potential μ and the hardness η become partial derivatives of the system's energy E expressed as a functional of an external potential $V(r)$, i.e., the nuclear conformation, and a function of the number of electrons N:

$$\mu = \left(\frac{\partial E}{\partial N}\right)_{V(r)} \tag{1}$$

$$\eta = \left(\frac{\partial^2 E}{\partial N^2}\right)_{V(r)} \tag{2}$$

The respective functional derivative with respect to $V(r)$ yields the electron density $\rho(r)$:

$$\rho(r) = \left(\frac{\delta E}{\delta V(r)}\right)_N \tag{3}$$

* E-mail: michael.beck@bayercropscience.com.

10.1021/ci049687n CCC: $30.25
Published on Web 02/16/2005

It can be shown that the hardness η becomes maximal for the density $\rho(r)$, which at a given $V(r)$ minimizes the energy E. The hardness is a global parameter related to chemical reactivity.

In a finite difference approach, the hardness can be approximated as

$$\eta \approx \frac{\mathrm{IP} - \mathrm{EA}}{2} \tag{4}$$

where

$$\mathrm{IP} = E[N-1, V(r)] - E[N, V(r)] \approx \mu^- \tag{5}$$

$$\mathrm{EA} = E[N, V(r)] - E[N+1, V(r)] \approx \mu^+ \tag{6}$$

are the vertical ionization potential and the vertical electron affinity, respectively.

Mulliken's electronegativity is

$$\chi = \frac{\mathrm{IP} + \mathrm{EA}}{2} \approx -\mu^0 \tag{7}$$

As indicated in eqs 5−7, IP, EA, and χ may be viewed as finite difference approximations to the left, right, and mean derivatives of the chemical potential, $\mu = (\partial E/\partial N)_{V(r)}$.

A local parameter of reactivity, the Fukui function, is obtained by a mixed derivative of the energy with respect to N and $V(r)$:

$$f^{\pm}(r) = \left(\frac{\delta^2 E}{\partial N \delta V(r)}\right)^{\pm} = \left(\frac{\partial \rho(r)}{\partial N}\right)^{\pm}_{V(r)} \tag{8}$$

Again the right derivative differs from the left derivative, as indicated by the ± sign.

Practically, the Fukui function is calculated by finite differences:

$$f^+(r) \approx \rho(N+1,r) - \rho(N,r)$$

$$f^-(r) \approx \rho(N,r) - \rho(N-1,r) \tag{9}$$

with all densities evaluated at a fixed external potential $V(r)$.

The maxima of f^+ indicate regions in the molecule, which prefer attack by a nucleophile, while f^- exhibits maxima at sites of preferred attack by an electrophile. Or, in other words, f^+ indicates where increase of electron density is energetically favorable, while f^- is maximal where decrease of electron density is preferred.

An equation that supports understanding of the interplay between global and local reactivity is

$$\mathrm{d}\mu = 2\eta\, \mathrm{d}N + \int \mathrm{d}r\, f(r)\, \mathrm{d}V(N,r) \tag{10}$$

which connects the change in chemical potential for the transition from one ground state to another to the changes in the number of electrons and the change in the external potential via the hardness and the Fukui function, respectively.

It should be noted that the Fukui functions in the definition adopted here restrict the description of reactivity to its electronic aspects. A more complete picture is gained by inclusion of nuclear displacement (see, for example, refs 29 and 30 and literature cited in these papers).

Why Fukui Functions May Be Related to Sites of Metabolism. As roughly sketched in the Introduction, metabolic hydroxylation mediated by cytochromes is attributed to a ferro-oxyl species (Cpd I). From present knowledge, Cpd I may be seen as an "electrophilic oxidant".[5] Thus the f^- function (calculated for the substrates) should help identify those places in a molecule, which prefer to be attacked by Cpd I. Conversely, the f^+ function, evaluated for Cpd I, should show where Cpd I prefers to be attacked by the substrate. Atomic HOMO coefficients from semiempirical calculations on agrochemicals have already been quite successfully correlated to oxidative metabolic paths.[31,32] (This procedure is essentially equivalent to calculate the f^- function in frozen orbital approximation, in which f^- reduces to the HOMO density).

The most blatant drawback of this kind of approach is obvious: The Fukui function describes reactivity against an isotropic, abstract "reactivity bath". If a drug experiences specific orientation in the active site of a cytochrome, the oxidation will not take place at the same site of the ligand as it would in an isotropic situation (e.g., in solution, with a small, sterically less demanding reaction partner). This is a common drawback of any "ligand based" approach.

METHODS

The following procedure was applied to all drugs in this study: A "reasonable" starting geometry was generated, which was optimized using the MMFF94s[33,34] force field as implemented in Sybyl.[35] The torsional conformational space was explored by an in-house method, which combines Monte Carlo steps and simulated annealing.[36] From the optimal conformations (in terms of MMFF94 energy), one was chosen manually. For some compounds, two to four geometries were investigated. The Fukui functions did not change significantly (i.e., the maxima were located at the same moieties across conformers). Thus, only one conformation will be reported in the following.

The selected conformations were subjected to full geometry optimization at RI-DFT level of theory.[37−39] The Becke−Perdew combination of functionals was employed.[40,41] Ahlrich's TZVP bases were assigned to all atoms.[42] Solvent effects were estimated using COSMO.[43] Dielectric constants of 80.2 (for water) and 4.0 (for the interior of an enzyme) were applied to estimate the difference between solution in water and the situation in a protein. Dielectric effects on global reactivity measures seem most pronounced for small dielectric constants $\epsilon < 4.0$.[44] Condensed Fukui functions show notable but not dramatic dielectric effects.[45,46] In the present calculations, the Fukui functions did not critically depend on the choice of dielectric constant; thus only results for $\epsilon = 4.0$ will be reported here. These, and all of the following DFT calculations, were performed using the Turbomole package of programs.[47]

At the geometry obtained so far, single-point unrestricted RI-DFT calculations were performed, using the same functionals and basis as before: One such calculation was done for the neutral species (N electrons), one for radical cation ($N-1$ electrons) and anion ($N+1$ electrons). Spin contamination was estimated via spin expectation values and

Table 1. Multiplicities (M) as Derived from the $\langle\langle S^2\rangle\rangle$ Expectation Values of the Individual Unrestricted RI-DFT/BP86/TZVP COSMO (ϵ = 4.0) Calculations[a]

object	M (anion)	M (neutral)	M (cation)	IP (kcal)	EA (kcal)	$-\mu^0 = \chi$ (kcal)	η (kcal)
adinazolam	2.0028	1.0000	2.0023	152.0	46.3	99.1	52.9
azelastine	2.0038	1.0000	2.0022	144.5	37.5	91.0	53.5
celecoxib	2.0021	1.0000	2.0023	161.6	43.8	102.7	58.9
Δ-8-tetrahydrocannabinol	2.0025	1.0000	2.0064	143.1	5.3	74.2	68.9
dexamethasone	2.0060	1.0000	2.0023	153.9	37.1	95.5	58.4
diclofenac	2.0027	1.0000	2.0053	142.9	21.8	82.4	60.6
estradiol-3-methyl ether	2.0038	1.0000	2.0037	146.2	4.9	75.6	70.7
etoposide	2.0024	1.0000	2.0023	135.3	16.0	75.7	59.6
felodipine	2.0023	1.0000	2.0100	146.2	38.0	92.1	54.1
flurbiprofen	2.0025	1.0000	2.0032	157.2	29.8	93.5	63.7
lorsatan	2.0026	1.0000	2.0034	152.8	28.8	90.8	62.0
MN-1695	2.0027	1.0000	2.0039	161.1	36.2	98.7	62.4
phenprocoumon	2.0030	1.0000	2.0033	154.5	39.4	96.9	57.6
phenytoin	2.0026	1.0000	2.0027	165.7	20.7	93.2	72.5
pranidipine	2.0032	1.0000	2.0068	143.4	53.6	98.5	44.9
S-MTPPA	2.0026	1.0000	2.0047	147.4	28.8	88.1	59.3
taxol	2.0038	1.0000	2.0010	154.5	36.4	95.5	59.0
warfarin	2.0031	1.0000	2.0036	153.8	37.4	95.6	58.2
capropamid	2.0041	1.0000	2.0019	163.1	15.4	89.2	73.9
chlorpyrifos	2.0037	1.0000	2.0024	189.5	7.0	98.2	91.3
fentrazamide	2.0030	1.0000	2.0022	165.5	30.5	98.0	67.5
imidacloprid	2.0030	1.0000	2.0033	165.9	36.7	101.3	64.6
iprovalicarb	2.0035	1.0000	2.0020	157.6	11.7	84.7	73.0
parathion	2.0028	1.0000	2.0034	198.6	20.5	109.6	89.0
propazin	2.0032	1.0000	2.0091	161.9	11.6	86.7	75.1
spirodiclofen	2.0044	1.0000	2.0018	166.1	28.7	97.4	68.7
spiroxamine	2.0009	1.0000	2.0020	139.2	15.2	62.0	77.2
thiabendazole	2.0039	1.0000	2.0050	149.9	33.8	92.0	58.0
thiacloprid	2.0039	1.0000	2.0093	167.0	32.8	99.9	67.1

[a] The right half of the table reports global reactivity parameters and multiplicities from all unrestricted DFT calculations as defined in eqs 4−7.

found to be reasonably small in all investigated cases (see Table 1).

The electron densities of the N and $N-1$ electron species were evaluated numerically on a regular grid of 0.5 Å resolution. The f^- Fukui functions were calculated from these grids by finite differences, see eq 9. Fukui functions were visualized using Molcad[48] (see Figure 2).

Table 1 also summarizes hardness values, electronegativities, ionization potentials, and electron affinities for the drugs evaluated here. These values are just provided for the sake of completeness; as this work does not aim at any quantitative prediction of metabolic rates or the like, these values will not be discussed any further.

The procedure was modified for Fukui calculations on Cpd I. In the calculations on the drugs, the N electron species are singlets, so the $N \pm 1$ electron species necessarily are doublets. According to the TSR model, the relevant spin states of Cpd I, however, are doublet (^2A) and quartet(^4A). When the N electron species has a multiplicity $M > 1$, addition of an electron may either lead to $M+1$ or $M-1$. The same is true for removal of an electron. Thus, in the absence of evidence ruling out either $M+1$ or $M-1$, two f^- and two f^+ Fukui functions for a given multiplicity $M > 1$ need to be considered, namely:

$$
\begin{aligned}
f_M^{+\uparrow}(r) &\approx \rho^{M+1}(N+1,r) - \rho^{M}(N,r)\\
f_M^{+\downarrow}(r) &\approx \rho^{M-1}(N+1,r) - \rho^{M}(N,r)\\
f_M^{-\uparrow}(r) &\approx \rho^{M}(N,r) - \rho^{M+1}(N-1,r)\\
f_M^{-\downarrow}(r) &\approx \rho^{M}(N,r) - \rho^{M-1}(N-1,r) \qquad (11)
\end{aligned}
$$

where the arrows $\uparrow$ and $\downarrow$ symbolize incrementation and decrementation of the multiplicity by one. $M = 2$ and 4 for the ^2A and ^4A states of Cpd I. On first sight, this kind of procedure might remind some readers of refs 50 and 51. These authors developed a theory of reactivity in $\{N, N_S, V(r)\}$ space, where $N_S = N_\alpha - N_\beta$. The resulting Fukui functions $f_{NN} = (\partial\rho/\partial N)_{N_S,V}$ and $f_{NS} = (\partial\rho/\partial N_S)_{N,V}$ are not to be confused with eq 11, which stay in the $\{N, V(r)\}$ picture.

To obtain the nucleophilic Fukui functions $f^{+\uparrow/\downarrow}$ for the Cpd I model system, the electron densities $\rho^1(N+1,r)$, $\rho^2(N,r)$, $\rho^3(N+1,r)$, $\rho^4(N,r)$, and $\rho^5(N+1,r)$ were obtained by single-point unrestricted RI-DFT/BP86 calculations for a model system of Cpd I. This was constructed from the QM/MM optimized geometry of the Cpd I protein complex calculated by Schöneboom et al.,[12] who kindly provided coordinate files. This calculation started from the experimental X-ray structure of CYP $P450_{cam}$.[52] All atoms were removed from this geometry except the heme moiety including the Fe═O group and the four protein residues closest to the sulfur bridge (residues CYS357, LEU358, GLY359, and GLN360) (Figure 1). Open valencies were filled with hydrogen atoms. COSMO was used for simulating a dielectric environment of $\epsilon = 4.0$. For the amino acids, SVP basis sets were used. The atoms comprising the tetrapyrrole system were assigned TZVP basis sets. TZVPP[42] was applied to the S—Fe═O moiety. To cope with the inner electrons of iron, the effective core potential method (ECP[53]) was used (ECP basis (8S7P6D)[6S5P3D][54]).

Unfortunately, the unrestricted calculations on the doublet state yielded densities with strong contamination by higher multiplets. The multiplicity derived from the $\langle\langle S^2\rangle\rangle$ expecta-

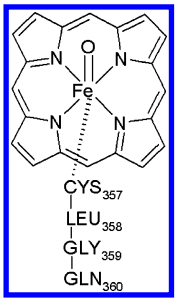

Figure 1. Model system for Cpd I.

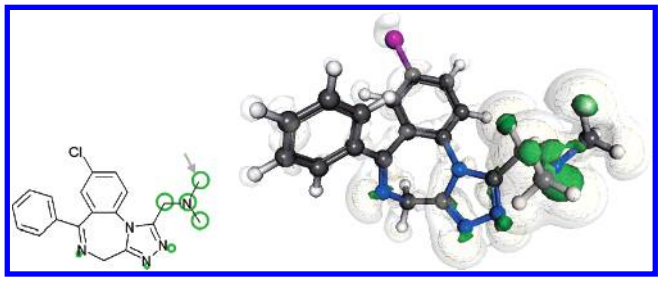

Figure 2. Electrophilic Fukui function f^- of adinazolam. Contour levels: 0.005 (green, opaque), 0.001 (yellow, net), 0.0005 (white, transparent). In this and the following figures, gray arrows indicate sites of metabolic hydroxylation. For reactions other than hydroxylation, these are either given explicitly or indicated by gray circles. Gray "lightning bolts" symbolize bond cleavage. The green circles are cartoons of the maxima of the f^- function. See text for details.

Table 2. Multiplicities Obtained in the Calculations on the Cpd I Model System[a]

electrons	target multiplicity	actual multiplicity
N	quartet	4.0123
N	doublet	2.8317
N	doublet*	2.0001
$N+1$	singlet	1.0001
$N+1$	triplet	3.0157
$N+1$	quintet	5.0243

[a] Note the huge spin contamination for the unrestricted calculation on the doublet state. The asterisk denotes that the calculation was performed using a spin annihilation technique, see text for details.

Table 3. Electron Affinities (in kcal) for the States Investigated on the Cpd I Model System[a]

participating states	singlet $N+1$	triplet $N+1$	quintet $N+1$
doublet* (N)	86.5	114.0	
quartet (N)		103.4	83.5

[a] Same nomenclature as in Table 2. For the neutral doublet state, only the energies from the spin projected calculation were considered.

tion value is 2.83 at the level of theory just sketched. As these contaminations are likely to spoil the Fukui functions derived from such densities, a spin annihilation technique[55,56] was applied to the unrestricted calculations on the doublet. Table 3 summarizes the obtained spin properties.

It is known[12,13] that the geometries of the quartet and the doublet state are very similar. Moreover, the propionic side chains of the porphyrin do not carry any substantial spin density. From these results, which were published after the calculations presented here had actually been performed, some justification is gained for the choice of model system. Indeed, the model system did not suffer from the drawbacks of other (especially gas-phase model systems) calculations, in which the distribution of spin density between the sulfur atom, the tetrapyrrole system and the Fe=O moiety differs qualitatively from the situation in the protein complex.[12,57]

Fukui functions were visualized as before. In addition, spin difference densities were calculated for the doublet and the quartet states:

$$\Delta\rho^M(N,r) = \rho^M(N_\alpha,r) - \rho^M(N_\beta,r) \qquad (12)$$

where $N = N_\alpha + N_\beta$, and it is assumed that $N_\alpha \geq N_\beta$.

RESULTS AND DISCUSSION

Drugs. Figure 3 shows the electrophilic Fukui function f^- for Adinazolam. For 17 further drugs, only cartoons of the electrophilic Fukui function are provided (see Figure 3). Visualizatons of all Fukui functions are available as Supporting Information. The ordering of the cartoons follows the order the respective drugs are discussed.

The first of the drug examples, adinazolam to taxol (Figures 2 and 3a−e), have been taken from Singh et al.[11] For these compounds, semiempirically estimated H-abstraction energies have been quite successfully correlated to sites of hydroxylation.[11] The remaining compounds (Figure 3f−q) have already been investigated by Zamora et al. using a 3D-QSAR model.[9]

A number of metabolites of adinazolam are known,[58] all of which result from attack on the tertiary amine, just as indicated by f^- (see Figure 2). The calculation for azelastine (Figure 3) correctly suggests similar reactions but overlooks hydroxylation at the 6-position.[59,60]

Out of the three main metabolites of diclofenac,[61] two correspond to f^- maxima, while the third hits a site between two maxima (Figure 3).

The most important metabolite of lorsartan, called E−3174,[62] is formed by oxidation of the CH_2OH group to the respective carboxylic acid. This is in line with f^- maxima near this group. However, in ref 9 two further oxidations are reported, hydroxylations of the butyl side chain. Of these two, only one corresponds to a tiny maximum of f^-.

The largest drug by far investigated here is taxol. For this drug, none of the reported metabolites[63] corresponds to a major f^- maximum. It is very unlikely that a molecule as large as this can freely rotate within any cytochrome's active site. Thus the sites of metabolism will be determined by steric constraints in the first place. If it is assumed that steric accessibility governs taxol's metabolism, and we secondly assume that the three phenyl rings are of similar accessibility, it is noteworthy that the hydroxylations at the terminal phenyl groups do correspond to f^- for very low contour levels; the phenyl with lowest f^- values is indeed not attacked at all (data not shown, see Supporting Information).

For phenytoin, correlation between the f^- function and observed metabolites is perfect.[64]

Felodipine shows a particularly rich manifold of metabolites.[65] Most involve oxidation of 1,4-dihydropyridine to pyridine, sometimes along with loss of one of the esters. While this is well reflected in f^-, hydroxylations at the methyl groups or the side chains of the esters cannot be related to f^-. The situation is the same for pranidipine.[66]

f^- of MN-1695 provides nice hints at the exchange of either one or both of the amines by oxygen, forming 1,3,5-triazine-2,4-dione or 1,3,5-triazine-2-one, respectively.[67]

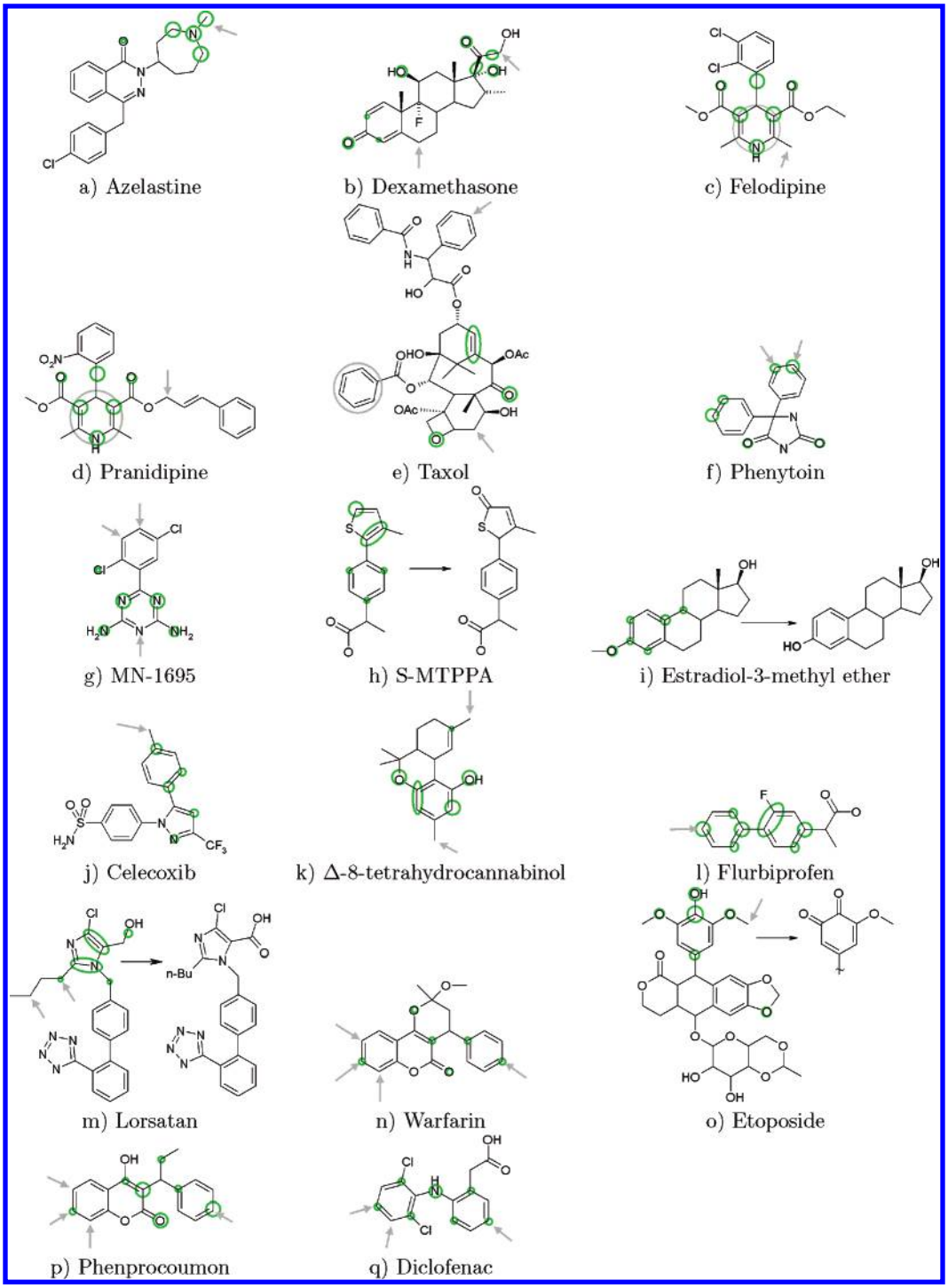

Figure 3. Cartoons of the electrophilic Fukui function f^- for 17 drugs. Gray arrows indicate sites of metabolic hydroxylation. For reactions other than hydroxylation, these are either given explicitly or indicated by gray circles. Gray "lightning bolts" symbolize bond cleavage. The green circles indicate maxima of the f^- function. See text for details.

However, the Fukui functions fail to predict hydroxylation at the phenyl. A further important metabolite is formed by N-oxidation at the 3-position of the triazine. From the Fukui function, one would have suspected the positions 1 or 5.

The Fukui function of etoposide has its most pronounced maxima at the bis-methoxy phenyl moiety. The major metabolites are indeed formed by attack in this region: demethylation and oxidation to *o*-benzoquinone.[68]

Hydroxylation products of Δ-8-tetrahydrocannabinol all result from attack at methyl groups. No metabolite corresponding to the f^- function is observed experimentally.[69]

The formation of a dihydro-5-oxo-2-thienyl compound from S-MTPPA[70] can be nicely correlated to f^-. However, again there is no strong hint in the f^- function at hydroxylation of a methyl group, which actual happens in vivo to the methyl group attached to the thiophene ring.[70] 4-Hydroxyflurbiprofen is the most prominent metabolite of flurbiprofen.[71] The Fukui function suggests some further sites of metabolism that, however, have not been observed.

As steroids are typically very specifically attacked metabolically,[4] one might not expect any correlation between a "ligand based" reactivity descriptor and observed metabolites.

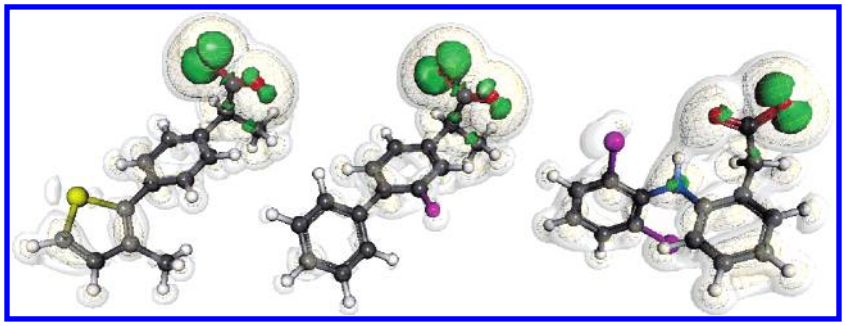

Figure 4. Electrophilic Fukui function f^- (left) calculated for the deprotonated forms of the acids S-MTPPA, flurbiprofen and diclofenac. Compare Figure 3. Contour levels: 0.005 (green, opaque), 0.001 (yellow, net), and 0.0005 (white, transparent).

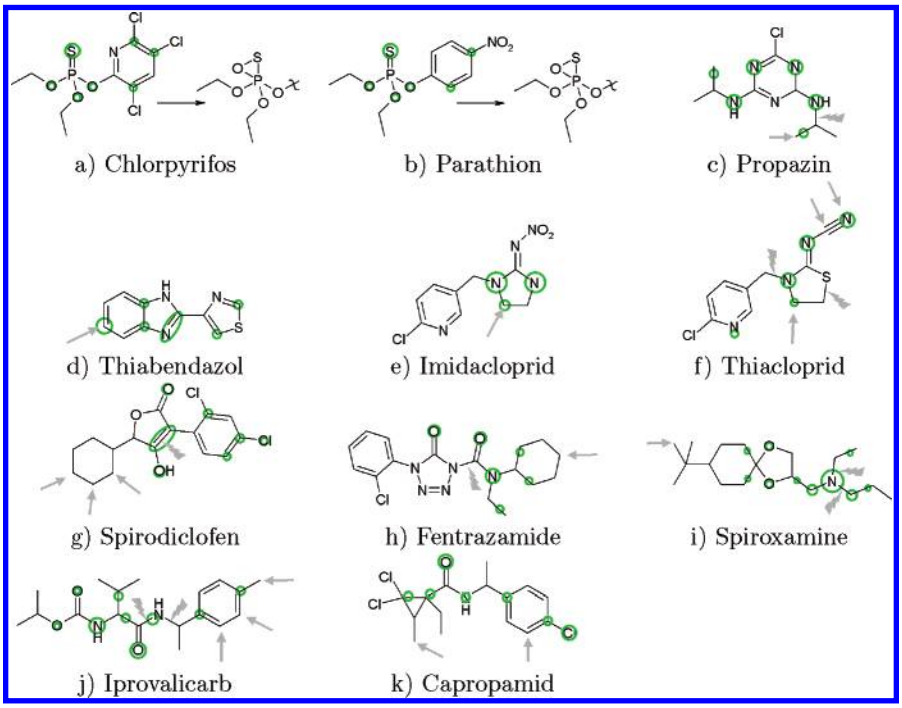

Figure 5. Cartoons of the electrophilic Fukui function f^- for 11 agrochemicals. Gray arrows indicate sites of metabolic hydroxylation. For reactions other than hydroxylation, these are either given explicitly or indicated by gray circles. Gray "lightning bolts" symbolize bond cleavage. The green circles indicate maxima of the f^- function. See text for details.

Surprisingly, for estradiol-3-methyl ether and dexamethasone one finds major metabolites[9,11] that can be related to f^- maxima. However, for a second major metabolite of dexamethasone, oxidation at one of the saturated six-membered rings, there is no corresponding maximum in the Fukui function.

Celecoxib experiences methyl hydroxylation.[72] There are maxima of f^- near to this group, but clear hints are missing. Celecoxib is an inhibitor of cytochrome P450 enzymes; thus the basic assumption of the current paper ("isotropic" reactivity) does not hold.

Phenprocoumon and warfarin also inhibit cytochromes. Following the argument just stated for celcoxib, no, or only poor correlation to observed metabolites should be expected. Surprisingly, all observed metabolites correspond to maxima of f^-.[73]

Two tautomers were calculated for phenprocoumon. The tautomer sketched in Figure 3 is preferred by ≈17 kcal/mol at RI-DFT/BP/TZVP/COSMO ($\epsilon = 4.0$) level of theory. Interestingly, the maxima of the Fukui function are at the same places in both tautomers, with the exception of the O═C─C═C─OH moiety, of course (result not shown).

Three of the investigated compounds are carboxylic acids (S-MTPPA, flurbiprofen, and diclofenac). It is likely that these compounds are deprotonated under physiological conditions. Moreover, it is known that some cytochrome P450s readily accept anions.[4] The f^- functions of the anions are shown in Figure 4. As expected, the electrophilic Fukui functions are concentrated at the carboxylate moiety, more or less ignoring the remaining parts of the molecules. Comparison of these functions to metabolites does not make much sense.

Agrochemicals. For agrochemicals, most metabolic studies have been performed in vivo. Only a few in vitro studies are available, for which the involvement of CYP P450 enzymes is proven. Discussion will start with four such examples: chlorpyrifos, propazin, parathion, and thiabendazole.[74−76] Again, only cartoons of the Fukui functions are provided (Figure 5a−d).

Chlorpyrifos and parathion in vitro metabolism in human microsomes is dominated by oxidative attack to the P═S double bond,[77] corresponding to the most prominent maxima of f^-.

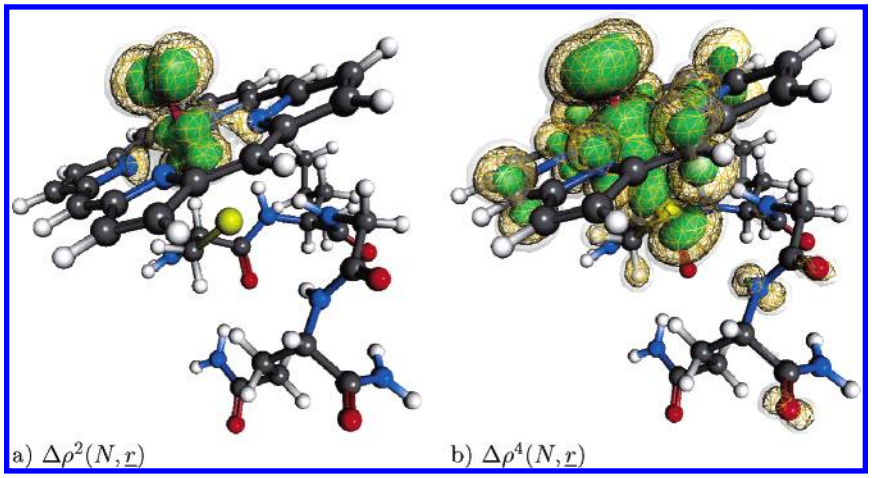

Figure 6. Spin densities of (a) the doublet and (b) the quartet state of the model system for Cpd I. Contour levels: 0.005 (green, opaque), 0.001 (yellow, net), and 0.0005 (white, transparent). Notation as in eq 12. See text for details.

Propazin experiences hydroxylation at the isopropyl groups and disruption of one or both of these groups by mammalian hepatic cytochrome P450 enzymes,[75] nicely reflected by f^-.

In mammalian cells, cytochromes hydroxylate thiabendazole[76] exactly as indicated by the largest f^- maximum.

For the following agrochemicals imidacloprid to capropamid (Figure 5e−k), in vitro metabolic studies are not available. Thus, it is not clear whether cytochromes are involved or not. Now the principal weakness of a ligand based approach, the disregard of the enzyme's structure, may become a strength: Whatever enzyme catalyzes formation of the observed metabolites, this enzyme may preferentially attack energetically favorable sites at the substrate (unless the substrate specifically binds into its pocket).

Imidacloprid undergoes hydroxylation exactly as indicated by its f^- function.[78] An analogous metabolite is observed for thiacloprid.[79] In addition to that, oxidation is observed at the nitrile. As for imidacloprid, f^- provides nice hints for these reactions.

Spirodiclofen carries an ester group, which is hydrolyzed readily in plants and animals.[80] Thus the f^- function was not calculated for spirodiclofen itself but for the hydrolysis product, a keto−enol. The two tautomers of this keto−enol differ by 5.8 kcal/mol at RI-DFT/BP/TZVP/COSMO (ϵ = 4.0) level of theory. Only the energetically preferred tautomer is discussed here. In animals, hydroxylation at the cyclohexane ring and oxidative opening of the keto−enol ring is observed.[80] While f^- shows activation at the enol double bond, distinctive features at the aliphatic ring are missing.

Fentrazamide's f^- function suggests attacks on aliphatic positions; however, none of these attacks are actually observed in vivo.[81] The observed metabolites, on the other hand, are not reflected by any f^- maximum.

Spiroxamine's tertiary amine undergoes N-oxidation, hydroxylation of the aliphatics attached to nitrogen, and degradation of the amine side chains,[82] just as indicated by f^-. Hydroxylation of the *tert*-butyl moiety could not be foreseen from inspection of f^-.

Iprovalicarb is a highly flexible molecule. The location of the f^- maxima are to a good approximation conformation independent. The amide group shows larger values of f^- than the O−C(=O)NH group, especially at the carbonyl oxygen. Indeed, bond cleavage is observed preferably at the amid.[83] The sites of hydroxylation at the toluyl moiety cannot be related to any major maxima.

The relation between capropamid's f^- and its observed metabolites is similarly poor.[84] There is a tiny maximum of f^- corresponding to hydroxylation of the phenyl in ortho-position to chlorine; however, this could easily be overseen. Again, there is no hint at all for hydroxylation of methyl group.

In summary, f^- maxima alone may not serve as a predictive tool for the estimation of metabolic sites of attack for drugs or agrochemicals. The metabolic reactions are far too complicated. The method particularly overlooks hydroxylations at aliphatic side chains. Hydroxylations at aromatic centers as well as other reactions (e.g., N-oxidation, bond cleavage, ...) very often coincide with f^- maxima. Semiempirical estimations of hydrogen abstraction energies[10,11] on the other hand, do not seem to have this problem with aliphatic side chains. But these calculations urgently need re-parameterization to find a balance between oxidations at aromatic and aliphatic centers. And of course, reactions such as N-oxidations cannot be predicted from H-abstraction energies.

Docking procedures have been quite successfully applied to the prediction of CYP mediated hydroxylations (e.g., ref 9). As Zamora et al. have pointed out in this paper, their approach does not take into account local reactivity at all, and this is suspected to be a major source of error. A docking procedure is thus very much complementary to the approach of this paper, in which protein specific interaction is neglegted. A combination of docking and local reactivity descriptors could indeed be an alternative to QM/MM modeling of metabolic reaction pathways. There is hope that such an approach could yield sufficient reliability at comparably low computational cost, thus allowing medium throughput calculations.

Cytochrome P450. The spin densities $\Delta\rho$ in Figure 6 a,b) show that the radical is more or less localized nearby the iron atom and its attached oxygen. In the doublet state, this behavior is more pronounced, as in the quartet a significant portion of spin density is found nearby sulfur and distributed over the tetrapyrrole perimeter. This is qualitatively in line with recent, more precise QM/MM findings.[5,13] From this, I draw the conclusion that the procedure (RI-DFT of the heme

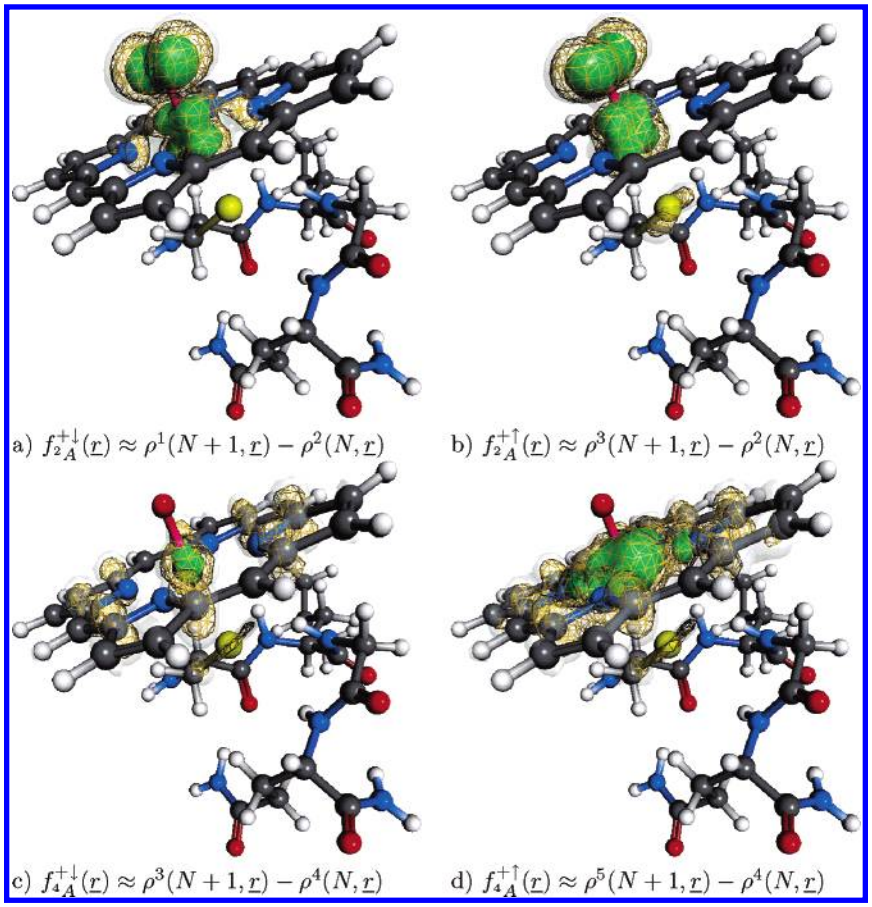

Figure 7. Nucleophilic Fukui functions of a model system for Cpd I. Panels a and b show the f^+ functions arising from a doublet state. Panels c and d are the respective functions arising from a quartet. The notation follows eq 11. See text for details.

plus a few amino acid residues embedded in a dielectric continuum) is sufficient to derive reasonable densities.

Inspection of the Fukui functions (Figure 7) shows that the reactivities derived from the quartet density $\rho^4(N,r)$ do not exhibit any maximum at the oxygen attached to the iron atom at all. $f_{4A}^{+\downarrow}$ is tightly localized around the iron atom. $f_{4A}^{+\uparrow}$, too, has its center around the iron but with significant side maxima at the pyrrole nitrogens. The Fukui functions derived from the doublet, $f_{2A}^{+\downarrow}$ and $f_{2A}^{+\uparrow}$, are very much localized at the Fe═O moiety and have a explicit maximum at the oxygen atom. Both functions comprise essentially an oxygen *p*-orbital and a iron *d*-orbital. Not surprisingly, the $f_{2A}^{+\downarrow}$ is very close to the spin density of the doublet ($\Delta\rho^2$) in Figure 6.

From the Fukui functions, one would draw the conclusion that the doublet has superior local reactivity at the Fe═O oxygen compared to the quartet. In refs 12 and 13, it is found that the doublet supplies a slightly energetically favorable route for oxidation via the rebound mechanism compared to the quartet. The more qualitative findings in this paper are in line with these results.

CONCLUSIONS

The electrophilic Fukui function f^- has been calculated for 18 drugs and 11 agrochemicals. Just for two drugs and two agrochemicals, no relation between the maxima of this function and observed metabolic reactions could be established. For the remaining compounds, one could indeed find agreement between theory and experiment. Metabolic reactions at aliphatic carbons are a notorious exception. Only seldom could *all* sites of metabolic attack be assigned to a maximum of the Fukui function.

Fukui functions should not be seen as a means of metabolism *prediction*. More precisely, these functions cannot help to predict which kind of reaction may occur. However, in close collaboration with experienced experts in metabolism, preferably (molecular) biologists, this theoretical concept may help to guide the search for metabolites, especially if the Fukui functions are "localized" (i.e., focused to some regions of a molecule).

The fundamental weakness of this ligand based approach, the disregard of any enzyme specific interactions, may also be viewed as a strength. Metabolism is not restricted to oxidation mediated by cytochromes, nor is it restricted to electrophilic attack. Fukui functions (f^- as well as f^+) may thus help to understand in vivo metabolic reactions of unknown enzymatic origin, as could be shown for five out of seven agrochemicals, for which no in vitro data were available.

The nucleophilic Fukui functions calculated for a model system of Cpd I are in qualitative agreement to sophisticated QM/MM results. This is encouraging, as it may motivate further work on the prediction of metabolic reactions; for this purpose, a combined docking/local reactivity approach could be a—less reliable but significantly cheaper—alternative to QM/MM studies on full reaction paths.

ACKNOWLEDGMENT

I thank Paul W. Ayers for "pre-reviewing" the manuscript and for constructive discussion. Jan Schöneboom kindly provided me with coordinate files from his first paper on CYP, which is gratefully acknowledged. Thanks to Thorsten Bürger and Svend Matthiessen, who greatly supported many of the calculations.

Supporting Information Available: Color figures of all computed Fukui functions. This material is available free of charge via the Internet at http://pubs.acs.org.

REFERENCES AND NOTES

(1) Greene, N. Computer systems for the prediction of toxicity: an update. *Adv. Drug Delivery Rev.* **2002**, *54*, 417−431.
(2) Langowski, J.; Long, A. Computer systems for the prediction of xenobiotic metabolism. *Adv. Drug Delivery Rev.* **2002**, *54*, 407−415.
(3) Winkler, D. A.; Burden, F. Toxicity modelling using Bayesian neural nets and automatic relevance detection. In *EuroQSAR 2002: Designing Drugs and Crop Protectants: Processes, Problems and Solutions*; Ford, M., Livingstone, D., Dearden, J., van de Waterbeemd, H., Eds.; Blackwell Publishing: Malden, MA, 2003; pp 251−254.
(4) Sono, M.; Roach, M. P.; Coulter, E. D.; Dawson, J. H. Heme-containing oxygenases. *Chem. Rev.* **1996**, *96*, 2841−2887.
(5) Shaik, S.; Cohen, S.; de Visser, S. P.; Sharma, P. K.; Kumar, D.; Kozuch, S.; Ogliaro, F.; Danovich, D. The "rebound controversy": An overview and theoretical modeling of the rebound step in C−H hydroxylation by cytochrome P450. *Eur. J. Inorg. Chem.* **2004**, 207−226.
(6) Cruciani, G.; Pastor, M.; Clementi, S.; Clementi, S. GRIND (grid independent descriptors) in 3D structure-metabolism relationships. In *Rational Approaches to Drug-Design, Proceedings of the European Symposium on Quantitative Structure−Activity Relationships 2000*; Hoeltje, H. D., Sippl, W., Eds.; Prous Science: Barcelona, Spain, 2001; pp 251−260.
(7) Afzelius, L.; Zamora, I.; Ridderstrom, M.; Andersson, T. B.; Karlen, A.; Masimirembwa, C. M. Competitive CYP2C9 inhibitors: Enzyme inhibition studies, protein homology modeling, and three-dimensional quantitative structure−activity relationship analysis. *Mol. Pharmacol.* **2001**, *59*, 909−919.
(8) de Groot, M. J.; Ekins, S. Pharmacophore modeling of cytochromes P450. *Adv. Drug Delivery Rev.* **2002**, *54*, 367−383.
(9) Zamora, I.; Afzelius, L.; Cruciani, G. Predicting drug metabolism: A Site of metabolism prediction tool applied to the Cytochrome P450 2C9. *J. Med. Chem.* **2003**, *46*, 2313−2324.
(10) Higgins, L.; Korzekwa, K. R.; Rao, S.; Shou, M.; Jones, J. P. An assesment of the reaction energetics for cytochrome P450-mediated reactions. *Arch. Biochem. Biophys.* **2001**, *385*, 220−230.
(11) Singh, S. B.; Shen, L. Q.; Walker, M. J.; Sheridan, R. P. A model for predicting likely sites of CYP3A4-mediated metabolism on drug-like molecules. *J. Med. Chem.* **2003**, *46*, 1330−1336.
(12) Schöneboom, J. C.; Lin, H.; Reuter, N.; Thiel, W.; Cohen, S.; Ogliaro, F.; Shaik, S. The elusive oxidant species of cytochrome P450: Characterization by QM/MM calculations. *J. Am. Chem. Soc.* **2002**, *124*, 8142−8151.
(13) Schöneboom, J. C.; Cohen, S.; Lin, H.; Shaik, S.; Thiel, W. Quantum mechanical/molecular mechanical investigation of the mechanism of C−H hydroxylation of camphor by cytochrome $P450_{cam}$: Theory supports a two-state rebound mechanism. *J. Am. Chem. Soc.* **2004**, *126*, 4017−4034.
(14) Groves, J. T.; Watanabe, Y. Reactive iron porphyrin derivatives related to the catalytic cycles of cytochrome P-450 and peroxidase. Studies of the mechanism of oxygen activation. *J. Am. Chem. Soc.* **1988**, *110*, 8443−8452.
(15) Roos, G.; Loverix, S.; De Proft, F.; Wyns, L.; Geerlings, P. A computational and conceptual DFT study of the reactivity of anionic compounds: implications for enzymatic catalysis. *J. Phys. Chem. A* **2003**, *107*, 6828−6836.
(16) Pearson, R. G. Hard and soft acids and bases. *J. Am. Chem. Soc.* **1963**, *85*, 3533−3539.
(17) Parr, R. G.; Yang, W. Density functional approach to the frontier-electron theory of chemical reactivity. *J. Am. Chem. Soc.* **1984**, *106*, 4049−4050.
(18) Parr, R. G.; Yang, W. *Density Functional Theory of Atoms and Molecules*; Clarendon Press: New York, 1989.
(19) Yang, W.; Parr, R. G.; Pucci, R. J. Electron density, Kohn−Sham frontier orbitals, and Fukui-functions. *J. Chem. Phys.* **1984**, *81*, 2862−2863.
(20) Ayers, P. W.; Parr, R. G. Variational principles for describing chemical reactions: The Fukui function and chemical hardness revisited. *J. Am. Chem. Soc.* **2000**, *122*, 2010−2018.
(21) Ayers, P. W.; Yang, W. Perpective on "Density functional approach to the frontier-electron theory of chemical reactivity". *Theor. Chem. Acc.* **2000**, *103*, 353−360.
(22) Pearson, R. G.; Parr, R. G. Absolute hardness: Companion parameter to absolute electronegativity. *J. Am. Chem. Soc.* **1983**, *105*, 7512−7516.
(23) Mulliken, R. S. New electroaffinity scale; together with data on valence states and on valance ionization potentials and electron affinities. *J. Chem. Phys.* **1934**, *2*, 782−789.
(24) Pauling, L. *Nature of the Chemical Bond*; Cornell University Press: Ithaca, NY, 1960.
(25) Sanderson, R. T. Electronegativities in inorganic chemistry. *J. Chem. Educ.* **1952**, *29*, 539−544.
(26) Hoffmann, R.; Woodward, R. G. Conservation of orbital symmetry. *Acc. Chem. Res.* **1968**, *1*, 17−22.
(27) Woodward, R. B.; Hoffmann, R. Die Erhaltung der Orbitalsymmetrie. *Angew. Chem.* **1969**, *21*, 797−869.
(28) Fukui, K. Role of fromtier orbitals in chemical reactions. *Science* **1982**, *218*, 747−754.
(29) Torrent-Sucarrat, M.; Duran, M.; Sola, M. Global Hardness evaluation using simplified models for the hardness kernel. *J. Phys. Chem. A* **2002**, *106*, 4632−4638.
(30) Torent-Sucarrat, M.; Luis, J. M.; Duran, M.; Toro-Labbe, A.; Sola, M. Relations among several nuclear and electronic density functional reactivity indices. *J. Chem. Phys.* **2003**, *119*, 9393−9400.
(31) Katagi, T. Application of molecular orbital calculations to the estimation of environmental and metabolic fates of pesticides. In *Rational Approaches to Structure, Activity and Ecotoxicology of Agrochemicals*; Fujita, W., Draber, T., Eds.; CRC Press: Boca Raton, FL, 1992; pp 543−564.
(32) Reid, D. L.; Calvitt, C. J.; Zell, M. T.; Miller, K. G.; Kingsmill, C. A. Early prediction of pharmaceutical oxidation by computational chemistry and forced degradation, *Pharm. Res.* **2004**, *21*, 1708−1717.
(33) Halgren, T. A. Merck Molecular Force Field. I−IV. *J. Comput. Chem.* **1996**, *17*, 491−641.
(34) Halgren, T. A. Merck molecular force field. VI−VII. *J. Comput. Chem.* **1999**, *20*, 720−748.
(35) *Sybyl Version 6.9.1*; Distributed by Tripos Inc.: St. Louis, MO, 2004.
(36) Bürger, Th. MOCCA: a conformational analysis tool combining Monte Carlo and Simulated Annealing techniques. Unpublished results.
(37) Eichkorn, K.; Treutler, O.; Oehm, H.; Haeser, M.; Ahlrichs, R. Auxiliary basis sets to approximate Coulomb potentials. *Chem. Phys. Lett.* **1995**, *240*, 283−290.
(38) Eichkorn, K.; Treutler, O.; Oehm, H.; Haeser, M.; Ahlrichs, R. Auxiliary basis sets to approximate Coulomb potentials. *Chem. Phys. Lett.* **1995**, *242*, 652−660.
(39) Eichkorn, K.; Weigend, F.; Treutler, O.; Ahlrichs, R. Auxiliary basis sets for main row atoms and their use to approximate Coulomb potentials. *Theor. Chem. Acc.* **1997**, *97*, 119−124.
(40) Perdew, J. P. Density functional approximation for the correlation energy of the inhomogenous electron gas. *Phys. Rev. B* **1086**, *33*, 8822−8824.
(41) Becke, A. D. Density functional exchange-energy approximation with correct asymptotic behaviour. *Phys. Rev. A* **1988**, *38*, 3098−3100.
(42) Jankowski, K.; Becherer, R.; Scharf, P.; Ahlrichs, R. The impact of higher polarization basis functions on molecular ab initio results. *J. Chem. Phys.* **1985**, *82*, 1413−1419.
(43) Klamt, A.; Schürmann, G. COSMO: A new approach to dielectric sreening in solvents with explicit expressions for the screening energy and its gradient. *J. Chem. Soc., Perkin Trans.* **1993**, *2*, 799−805.
(44) Li, P.; Bu, Y.; Ai, H. Theoretical determinations of ionization potential and electron affinioty of glycinamide using DFT. *J. Phys. Chem. A* **2004**, *108*, 1200−1207.
(45) Safi, B.; Balawender, R.; Geerlings, P. Solvent effects on electronegativity, hardness, condensed fukui functions, and softness, in a large series of diatomic and small polyatomic molecules: Use of the EFP model. *J. Phys. Chem.* **2001**, *105*, 11102−11109.
(46) Balawender, R.; Safi, B.; Geerlings, P. Solvent effects on the global and atomic DFT-based reactivity descriptors using the effective fragment potential model. Solavation of ammonia. *J. Phys. Chem. A* **2001**, *105*, 6703−6710.
(47) Ahlrichs, R.; Bär, M.; Baron, H.-P.; Bauernschmitt, R.; Böcker, S.; Ehrig, M.; Eichkorn, K.; Elliott, S.; Furche, F.; Haase, F.; Häser, M.; Horn, H.; Hättig, Ch.; Huber, Ch.; Huniar, U.; Kattannek, M.; Köhn, A.; Kölmel, Ch.; Kollwitz, M.; May, K.; Ochsenfeld, Ch.; Öhm, H.; Schäfer, A.; Schneider, U.; Treutler, O.; Tsereteli, K.; Unterreiner, B.; von Arnim, M.; Weigend, F.; Weis, P.; Weiss, H. *Turbomole Version 5.6*; Universität Karlsruhe: Karlsruhe, Germany, 2002.
(48) Keil, M.; Exner, T.; Brickmann, J. *Molcad II* (*Mk*) *v1.4.16*; Distributed by Tripos Inc.: St, Louis, MO, 2004.

(49) Mulliken, R. S. Electronic population analysis on LCAO-MO molecular wave functions. I−IV. *J. Chem. Phys.* **1955**, *23 (10)*, 1833−1846, 2338−2346.
(50) Vargas, R.; Cedillo, A.; Garza, J.; Galvan, M. Reactivity criteria in spin polarized density functional theory. In *Reviews in Modern Quantum Chemistry: A Celebration of the Contributions of Robert Parr*; Sen, K., Ed.; World Scientific: Singapore, 2002; pp 936−965.
(51) Melin, J.; Aparicio, F.; Fuentealba, P.; Contreras, R. Chemical reactivity in the $\{N, N_S, \nu(\mathbf{r})\}$ space. *J. Phys. Chem. A* **2003**, *107*, 3831−3835.
(52) Schlichting, I.; Berendzen, J.; Chu, K.; Stock, A. M.; Maves, S. A.; Benson, D. A.; Sweet, R. M.; Ringe, D.; Petsko, G. A.; Sligar, S. G. The catalytic pathway of cytochrome P450cam at atomic resolution. *Science* **2000**, *287*, 1615−1622.
(53) Wahlgren, U. The effective core potential method. In *Lecture Notes in Quantum Chemistry: European Summer School in Quantum Chemistry*; Roos, B. J., Ed.; Springer Verlag: Berlin, Germany, 1992; pp 413−421.
(54) Dolg, M.; Wedig, U.; Stoll, H.; Preuss, H. Energy-adjusted ab initio speudopotentials for the first row transition elements. *J. Chem. Phys.* **1987**, *86*, 866−872.
(55) Szabo, A.; Ostlund, N. S. *Modern Quantum Chemistry: Introduction to Advanced Electronic Structure Theory*; McGraw-Hill: New York, 1982.
(56) McWeeny, R. *Methods of Molecular Quantum Mechanics*; Academic Press: New York, 1978.
(57) Ogliaro, F.; Cohen, S.; Filatov, M.; Harris, N.; Shaik, Sason. The high-valent compound of cytochrome P450: The nature of the Fe−S bond and the role of the thiolate ligand as an internal electron donor. *Angew. Chem., Int. Ed.* **2000**, *39*, 3851−3855.
(58) Sethy, V. H.; Collins, R. J.; Daniels, E. G. Determination of biological activity of adinozolam and its metabolites. *J. Pharm. Pharmacol.* **1984**, *36*, 546−548.
(59) Nakajima, M.; Ohyama, K.; Nakamura, S.; Shimada, N.; Yamazaki, H.; Yokoi, Tsuyoshi. Inhibitory effects of azelastine and its metabolites on drug oxidation catalyzed by human cytochrome P-450 enzymes. *Drug Metab. Disp.* **1999**, *27*, 792−797.
(60) Imai, T.; Taketani, M.; Suzu, T.; Kusube, K.; Otagiri, M. In vitro identification of the human cytochrome P-450 enzymes involved in the N-demethylation of azelastine. *Drug Metab. Disp.* **1999**, *27*, 942−946.
(61) Dorado, P.; Berecz, R.; Noberto, M.-J.; Yasar, U.; Dahl, M.-L.; Lerena, A. CYP2C9 genotypes and diclofenac metabolism in Spanish healthy volunteers. *Eur. J. Clin. Pharmacol.* **2003**, *59*, 221−225.
(62) Suzuki, J.; Ohta, H.; Hanada, K.; Kawai, N.; Ikeda, T.; Nakao, M.; Ikemoto, F.; Nishikibe, M. Acute effects of E-3174, a human active metabolite of losartan, on the cardiovascular system in tachycardia-induced canine heart failure. *Hypertens. Res.* **2001**, *24*, 65−74.
(63) Desai, P. B.; Duan, J. Z.; Zhu, Y.-W.; Kouzi, S. Human liver microsomal metabolism of paclitaxel and drug interactions. *Eur. J. Drug Metab. Pharmacokinet.* **1998**, *23*, 417−424.
(64) Mamiya, K.; Ieiri, I.; Shimamoto, J.; Yukawa, E.; Imai, J.; Ninomiya, H.; Yamada, H.; Otsubo, K.; Higuchi, S.; Tashiro, N. The effects of genetic polymorphisms of CYP2C9 and CYP2C19 on phenytoin metabolism in Japanese adult patients with epilepsy: Studies in stereoselective hydroxylation and population pharmacokinetics. *Epilepsia* **1998**, *39*, 1317−1323.
(65) Wang, S. X.; Sutfin, T. A.; Baeaernhielm, C.; Regaardh, C. G. Contribution of the intestine to the first-pass metabolism of felodipine in the rat. *J. Pharmacol. Exp. Ther.* **1989**, *250*, 632−636.
(66) Sasabe, H.; Futaki, N.; Matsuki, K.; Morita, S.; Uchida, M.; Miyamoto, G.; Odomi, M. Metabolic fate of pranidipine. (IV). Metabolism of pranidipine, a new dihydropyridine calcium antagonist, and identification of metabolites in rats, dogs and human. *Iyakuhin Kenkyu* **1993**, *24*, 1101−1114.
(67) Ueda, F.; Hara, K.; Mimura, K.; Yano, T.; Kyoi, T.; Kimura, K.; Nomura, A.; Enomoto, H. Pharmacological and toxicological studies on 2,4-diamino-6-(2,5-dichlorophenyl)-*s*-triazine maleate (MN-1695) and its metabolites and decomposition products: acute toxicity, effects on smooth muscles and antiulcer effects. *Oyo Yakuri* **1986**, *32*, 861−871.
(68) Lovett, B. D.; Strumberg, D.; Blair, I. A.; Pang, S.; Burden, D. A.; Megonigal, M. D.; Rappaport, E. F.; Rebbeck, T. R.; Osheroff, N.; Pommier, Y. G.; Felix, C. A. Etoposide metabolites enhance DNA topoisomerase II cleavage near leukemia-associated MLL translocation breakpoints. *Biochemistry* **2001**, *40*, 1159−1170.
(69) Brown, N. K.; Harvey, D. J. In vivo metabolism of the methyl homologues of delta-8-tetrahydrocannabinol, delta-9-tetrahydrocannabinol and abn-delta-8-tetrahydrocannabinol in the mouse. *Biomed. Environ. Mass Spectrosc.* **1988**, *15*, 389−398.
(70) Taguchi, K.; Konishi, T.; Nishikawa, H.; Kitamura, S. Identification of human cytochrome P450 isoforms involved in the metabolism of S-2-[4-(3-methyl-2-thienyl)phenyl]propionic acid. *Xenobiotica* **1999**, *29*, 899−908.
(71) Hutzler, J. M.; Hauer, M. J.; Tracy, T. S. Dapsone activation of CYP2C9-mediated metabolism: evidence for activation of multiple substrates and a two-site model. *Drug Metab. Disp.* **2001**, *29*, 1029−1034.
(72) Tang, C.; Shou, M.; Rushmore, T. H.; Mei, Q.; Sandhu, P.; Woolf, E. J.; Rose, M. J.; Gelmann, A.; Greenberg, H. E.; DeLepeleire, I.; VanHecken, A.; DeSchepper, P. J.; Ebel, D. L.; Schwartz, J. I.; Rodrigues, A. D. In-vitro metabolism of celecoxib, a cyclooxygenase-2 inhibitor, by allelic variant forms of human liver microsomal cytochrome P450 2C9: Correlation with CYP2C9 genotype and in-vivo pharmacokinetics. *Pharmacogenetics* **2001**, *11*, 223−235.
(73) Yamazaki, H.; Inoue, K.; Chiba, K.; Ozawa, N.; Kawai, T.; Suszuki, Y.; Goldstein, J. A.; Guenrich, F. P.; Shimada, T. Comparative study on the catalytic roles of cytochrome P450 2C9 and its Cys- and Leu-Variants in the oxidation of warfarin, flurbiprofen, and diclofenac by human liver microsomes. *Biochem. Pharmacol.* **1998**, *56*, 243−251.
(74) Hodgson, E. In vitro human phase I metabolism of xenobiotics I: Pesticides and related chemicals used in agriculture and public health, September 2001. *J. Biochem. Mol. Toxicol.* **2001**, *15*, 296−299.
(75) Hanioka, N.; Jinno, H.; Tanaka-Kagawa, T.; Nishimura, T.; Ando, M. In vitro metabolism of simazine, atrazine and propazine by hepatic cytochrome P450 enzymes of rat, mouse and guinea pig, and estrogenic activity of chlorotriazines and their main metabolites. *Xenobiotica* **1999**, *29*, 1213−1226.
(76) Coulet, M.; Eeckhoutte, C.; Larrieu, G.; Sutra, J.-F.; Alvinerie, M.; Mace, K.; Pfeifer, A.; Zucco, F.; LauraStammati, A.; DeAngelis, I.; Vignoli, A. L.; Galtier, P. Evidence for cytochrome P4501A2-mediated protein covalent binding of thiabendazole and for its passive intestinal transport: use of human and rabbit derived cells. *Chem.-Biol. Interact.* **2000**, *127*, 109−124.
(77) Hodgson, J. ADMET-turning chemicals into drugs. *Nat. Biotechnol.* **2001**, *19*, 722−726.
(78) Krohn, J.; Hellpointer, E. Environmental fate of imidacloprid. *Pflanzenschutz-Nachr. Bayer* **2002**, *55*, 3−25.
(79) Klein, O. Behaviour of thiacloprid (YRC2894) in plants and animals. *Pflanzenschutz-Nachr. Bayer* **2001**, *54*, 209−239.
(80) Koester, J. Metabolism of spirodiclofen (BAJ 2740) in animals and plants. *Pflanzenschutz-Nachr. Bayer* **2002**, *55*, 237−254.
(81) Koester, J. Metabolism of fentrazamide (YRC 2388) in plants and animals. *Pflanzenschutz-Nachr. Bayer* **2001**, *54*, 51−74.
(82) Klein, O.; Reiner, H.; Scholz, K. Metabolism and residues of Spiroxamine (KWG 4168) in plants, animals and the environment. *Pflanzenschutz-Nachr. Bayer* **1997**, *50*, 71−98.
(83) Anderson, C. Metabolism of iprovalicarb (SZX 0722) in animals. *Pflanzenschutz-Nachr. Bayer* **1999**, *52*, 85−96.
(84) Kurogochi, S.; Köster, J. Metabolism and residues of carpropamid (KTU 3616) in plants, animals and the environment. *Pflanzenschutz-Nachr. Bayer* **1998**, *51*, 221−246.

CI049687N